Bull. Soc. géol. France, 2015, t. 186, n° 1, pp. 3-19

SI-Hex: a new catalogue of instrumental seismicity for metropolitan France

MICHEL CARA[1], YVES CANSI[2], ANTOINE SCHLUPP[1], PIERRE ARROUCAU[4], NICOLE BÉTHOUX[3], ERIC BEUCLER[4], STÉPHANE BRUNO[2], MARIE CALVET[5], SÉBASTIEN CHEVROT[6], ALEXANDRA DEBOISSY[1], BERTRAND DELOUIS[3], MARYLIN DENIEUL[1], ANNE DESCHAMPS[7], CÉCILE DOUBRE[1], JULIEN FRÉCHET[8], STÉPHANIE GODEY[9], OLIVIA GOLLE[4], MARC GRUNBERG[1], JOCELYN GUILBERT[2], MÉRIC HAUGMARD[4], LILIANE JENATTON[10], SOPHIE LAMBOTTE[1], DELPHINE LEOBAL[2], CHRISTOPHE MARON[3], VÉRONIQUE MENDEL[8], SOPHIE MERRER[2], MARIE MACQUET[4], ARNAUD MIGNAN[1], ANTOINE MOCQUET[4], MARC NICOLAS[2], JULIE PERROT[11], BERTRAND POTIN[10], OLIVIER SANCHEZ[10], JEAN-PAUL SANTOIRE[2], OLIVIER SÈBE[2], MATTHIEU SYLVANDER[5], FRANÇOIS THOUVENOT[10], JÉRÔME VAN DER WOERD[8] and KATIA VAN DER WOERD[1]

Keywords. – Seismicity, Magnitude, Discrimination, Seismic hazard, Seismotectonics, France.

Abstract. – The aim of the SI-Hex project (acronym for « Sismicité Instrumentale de l'Hexagone ») is to provide a catalogue of seismicity for metropolitan France and the French marine economic zone for the period 1962-2009 by taking into account the contributions of the various seismological networks and observatories from France and its neighbouring countries. The project has been launched jointly by the Bureau Central Sismologique Français (CNRS-University/BCSF) and the Laboratoire de Détection et de Géophysique (CEA-DAM/LDG). One of the main motivations of the project is to provide the end user with the best possible information on location and magnitude of each earthquake. So far, due to the various procedures in use in the observatories, the different locations and magnitudes of earthquakes located in the SI-Hex zone were presenting large discrepancies. In the 2014 version of the catalogue, 1D localizations of hypocentres performed with a unique computational scheme and covering the whole 1962-2009 period constitute the backbone of the catalogue (SI-Hex solutions). When available, they are replaced by more precise localizations made at LDG or, for recent times, by the regional observatories within: 1) the French Alps, 2) the southernmost Alps and the Mediterranean domain including Corsica, 3) the Pyrenees, and 4) the Armorican massif. Moment magnitudes M_w are systematically reported in the SI-Hex catalogue. They are computed from coda-wave analysis of the LDG records for most M_w>3.4 events, and are converted from local magnitudes M_L for smaller magnitude events. Finally, special attention is paid to the question of discrimination between natural and artificial seismic events in order to produce a catalogue for direct use in seismic hazard analysis and seismotectonic investigations. The SI-Hex catalogue is accessible on the web site *www.franceseisme.fr* and contains 38,027 earthquake hypocentres, together with their seismic moment magnitudes M_w.

SI-Hex : nouveau catalogue de sismicité instrumentale de la France métropolitaine

Mots-clés. – Sismicité, Magnitude, Discrimination, Aléa sismique, Sismotectonique, France.

Résumé. – Le but du projet SI-Hex – "Sismicité Instrumentale de l'Hexagone" – est de créer un catalogue de sismicité de la France métropolitaine et de la zone exclusive économique en mer (ZEE) sur la période 1962-2009 à partir des données provenant des observatoires et réseaux sismologiques français, complétées par celles des pays voisins. Le projet a été lancé conjointement par le Bureau Central Sismologique Français (Université-CNRS/BCSF) et le Laboratoire de Détection et de Géophysique (CEA-DAM/LDG). L'une des motivations principales est de fournir à l'utilisateur la meilleure information possible sur la localisation et la magnitude de chaque séisme. Jusqu'à présent, à cause des procédures variées utilisées par les observatoires, les localisations et les magnitudes des séismes localisés dans la zone SI-Hex présentent d'importants écarts. Dans la version 2014 du catalogue, les localisations 1D des hypocentres effectuées avec un schéma de calcul unique et couvrant l'ensemble de la période 1962-2009 constituent l'épine dorsale du catalogue (solutions SI-Hex). Lorsque des solutions plus précises existent, ces dernières sont substituées aux localisations SI-Hex. C'est le cas pour certaines localisations faites par le LDG, ou aux périodes récentes par les observatoires régionaux en ce qui concerne : 1) les Alpes françaises, 2) le sud des Alpes et le domaine méditerranéen incluant la Corse, 3) les Pyrénées et 4) le Massif armoricain. Les magnitudes de moment M_w sont systématiquement reportées dans le catalogue SI-Hex. Elles sont calculées à partir d'une analyse des ondes de coda enregistrées par le LDG pour la plupart des séismes de magnitude M_w>3,4 et sont converties à partir des magnitudes locales M_L pour les séismes de plus petites magni-

1. Université de Strasbourg, EOST, UMR 7516, 5 rue R. Descartes, 67084 Strasbourg cedex
2. CEA, Bruyères Le Chatel, DAM/DIF/LDG, 91297 Arpajon
3. Université de Nice-Sophia-Antipolis, OCA, UMR 6526, 250 rue Albert Einstein, 06560 Valbonne
4. Université de Nantes, IUEM, UMR 6112, 2 rue de la Houssinière, BP 92208, 44322 Nantes cedex 3
5. Université Paul Sabatier, OMP, UMR 5562, 14 av. Edouard Belin, 31400 Toulouse
6. CNRS, OMP, UMR 5562, 14 av. Edouard Belin, 31400 Toulouse
7. CNRS, OCA, UMR 6526, 250, rue Albert Einstein, 06560 Valbonne
8. CNRS, EOST, UMR 7516, 5 rue R. Descartes, 67084 Strasbourg cedex
9. CSEM, c/o CEA, Bt. Bard, Centre DAM-Ile de France, 91297 Arpajon cedex
10. Université Joseph Fourier, OSUG, UMR 5559, 1381 Rue de la piscine, BP 53, 38041 Grenoble cedex 9
11. Université de Bretagne Occidentale, IUEM, UMR 6538, Place Nicolas Copernic, 29280 Plouzané
Manuscript deposited on July 7, 2014; accepted on October 15, 2014

tudes. Finalement, une attention particulière a été apportée à la question de la discrimination entre séismes naturels et artificiels afin de produire un catalogue directement utilisable pour les analyses d'aléa sismique et les études de sismotectonique. Le catalogue SI-Hex est accessible sur le site web *www.franceseisme.fr* et contient 38 027 hypocentres de séisme, chacun avec sa magnitude de moment M_w.

INTRODUCTION

Several catalogues of seismicity based on different seismic networks and different processing techniques have been produced in France over the past 50 years. The SI-Hex project was launched in 2009 in order to produce a new catalogue of seismicity for metropolitan France with accurate hypocentre locations and moment magnitude determinations. In contrast with all the previous French catalogues of seismicity, this collaborative project makes use of the original data coming from several regional and national seismic networks operating in metropolitan France, together with parametric data coming from the surrounding European networks. SI-Hex covers the period 1962-2009 and is designed as a tool for seismic hazard analysis and seismotectonics study.

Since 1962, a constant effort has been pursued by LDG (Laboratoire de Détection et de Géophysique of CEA, Commissariat à l'énergie atomique et aux énergies alternatives) in order to publish a catalogue based on homogeneous procedures for hypocentre and magnitude determinations. Since those early times, the LDG seismic telemetric network has been covering the whole metropolitan France with high sensitivity 1-Hz velocity sensors well adapted to both teleseismic and local earthquake detections. This network was the first centralized facility for monitoring seismicity in France. At those early times, it complemented the sparse network of stations belonging to academic institutions.

Since the 1970s, local and regional seismic networks have progressively been developed by academic institutions in the most seismically active regions of France (for institution acronyms definition, see Appendix A). These additional networks were the result of initiatives associating several Universities and CNRS, the French National Centre for Scientific Research. The first such initiative came from IPGS (Strasbourg) with the development of telemetric networks in the early 1970s. It helped improving the monitoring of seismicity in different regions: northeastern France, the southeastern Alpine region near Nice, and around the gas field of Lacq near Pau. At the end of the 1970s, IPGP (Paris) deployed a local network in the Pyrenees near Arette, a locality struck by a damaging earthquake in 1967. In the 1980s, the central and northern French Alps were equipped by LGIT (Grenoble) with a regional phone-transmission system (Sismalp network), while at the same time IPGS installed a new local network in Provence near Marseille, and OMP (Toulouse) started the deployment of a regional network in the Pyrenees. Decision to gather the data coming from theses different networks has been taken by INSU-CNRS, with the launch of RéNaSS (Réseau National de Surveillance Sismique [Aubert *et al.*, 1982; Cara *et al.*, 1986]). The RéNaSS headquarter has been installed at BCSF (Bureau Central Sismologique Français), the national academic bureau for seismology depending on the University of Strasbourg since 1921. With some additional stations installed in western France and in the Massif Central by teams from Strasbourg (IPGS) and Clermont-Ferrand (OPGC), the number of short-period velocity sensors participating in seismicity monitoring of metropolitan France was larger than 100 in the early 1990s.

The next decisive steps for seismicity monitoring are taken in the late 1990s with the initiative of LGIT (Grenoble) in order to complement the various high-sensitivity velocimetric networks with a permanent strong motion network (RAP), a large multi-partner project. It is aimed at deploying a broad network of homogeneous sensors with a wide dynamic range recording system [Pequegnat *et al.*, 2008]. Independently, a great improvement occurred in 1997 at LDG with a satellite transmission recording system, while efforts from academic laboratories led them to start the deployment of broadband high-dynamic-range stations.

By now these collaborative efforts are merged into the RESIF project, a new consortium which aims at developing both seismic and geodetic networks to monitor the ground motion in metropolitan France with instruments reaching the best international quality standards (*http://www.resif.fr*).

The SI-Hex project directly relies on the data available from the seismic networks developed since 1962. Accuracy of magnitude and hypocentre locations, in conjunction with the quality of the discrimination made between natural and artificial seismic sources are thus uneven along the years covered by the SI-Hex project. In the following, we show how the different steps of the SI-Hex project allowed us to take into account the evolutions of the French seismic networks since 1962 in order to produce the catalogue. Identification of events is made by constructing first a backbone catalogue based on homogeneous procedures and on multi-origin sources of data including events seen only by the regional French networks, and in a second step, it is complemented with more accurate locations from the regional observatories.

HYPOCENTRE LOCATION

The geographical target of SI-Hex is an area covering the whole metropolitan France including the marine zone encompassing the whole French exclusive economic area. An extension of 20 km off these contours is added in order to account for the largest uncertainties in the epicentre location. This geographical area is referred to as the "SI-Hex zone". In the process of construction of the 1962-2009 backbone catalogue described below, computation of epicentres was extended to the geographic frame [41°N, 52°N; 6°W, 10°E] for all the events detected by at least one of the French seismic networks. This extended area is referred to as the "extended SI-Hex zone".

The backbone catalogue: homogeneous location procedure in the extended SI-Hex zone

The first task of the project was to produce a catalogue for the whole SI-Hex zone by merging the arrival times from

the French networks and those from the foreign stations provided by EMSC [Godey *et al*., 2013], the Euro-Mediterranean Seismological Centre, and by ISC, the International Seismological Centre. Before 1978, hypocentre locations mainly rely on the reading of arrival-times on the LDG multi-trace paper records and on bulletin data from abroad observatories (fig. 1a). Additional stations installed during the following two decades allowed to gradually improve the accuracy of hypocentre locations. Figure 1b shows the contributing stations during the period 1998-2005.

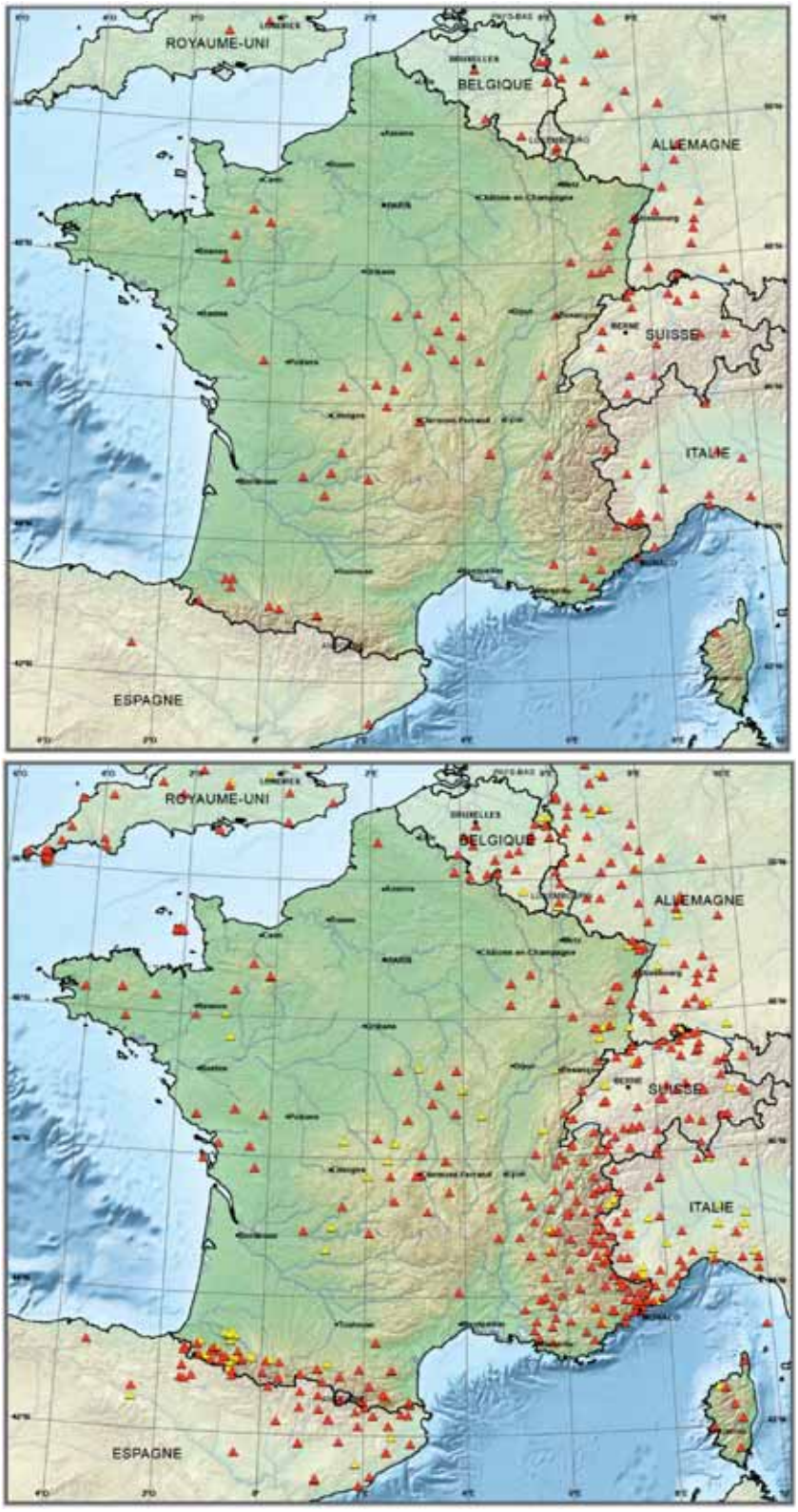

FIG. 1. – Short-period seismic stations contributing to the SI-Hex backbone catalogue in two periods: a) [1962-1977]; and b) [1998-2005]. Red triangles are stations used in the hypocentre localization during indicated period and yellow triangles show the stations no longer active after 1997.

The collected set of 3,261,922 arrival times data were merged with the CEA-LDG computation code "Fusion". It produced a number of 110,480 seismic events in the extended SI-Hex zone. Hypocentre localization is based on an iterative damped least square linearized inversion. Regional crustal phases Pn, Pg, Sn and Sg (or Lg) are taken into account when possible. If not, P- or S-waves, reported at some stations as first arrivals, are used. Phase identification relies on the computations made with a 1D velocity model of the crust and upper mantle, based on a simplified version of the Haslach model used by RéNaSS (table I).

In order to take into account the different seismic data (arrival times and back azimuths) they are weighted in such a way that P arrival times are favoured in the location process (residuals between the observed and predicted data are weighted by a factor 1 for P, 0.5 for S, and 1/30° for azimuths). No weight based on epicentral distance is applied to the data in the backbone catalogue, unlike the procedures applied for the regional catalogues for which the nearest stations are favoured. A statistical analysis of arrival time residuals is performed in order to reject outliers from the set of arrival time data before the final localization.

Except in some cases where a station is close to the epicentre, the hypocentral depth is poorly resolved. In the preliminary steps of the iterative inversion process, epicentres, origin times and depths are computed. When the process fails, inversion is performed for a series of fixed depths sampling the crust and the upper mantle. If there is a significant RMS (Root Mean Square) minimum, the depth is set to this value, if not, the depth is set by the analyst at a standard value. Note that in this computational process, some depths cluster at the bottom of the first layer of the velocity model at 20 km depth (table I).

Due to the evolution of the station distribution between 1962 and 2009, and due to the improvement of the seismic phase picking techniques, RMS precision of the location – hereafter referred to as computational errors – improved with time. Figure 2 shows that prior to 1977 computational errors larger than 20 km are expected in many places for small magnitude earthquakes and in some areas, such as the Ligurian margin off the coast of the French Riviera (fig. 2a). The situation is much better in recent times with the largest computational errors expected in the Atlantic ocean and Corsica. Note that the computational error should not be misunderstood as being the location accuracy. The bias due to the localization procedure may be larger than the computational errors shown in figure 2. Few comparisons with accurately located or relocated epicentres after monitoring aftershock sequences with temporary local networks, show that such biases should not excess 10 km in most regions of the continental SI-Hex zone, but they can be larger outside this area within the extended SI-Hex zone. Another important point concerns the dependence of location computational errors upon magnitudes: because a larger magnitude makes the number of involved stations larger, the azimuthal coverage is improved, and the computational errors may decrease.

Regional hypocentre locations: preferential SI-Hex solutions

In order to improve the accuracy in epicentre location and hypocentre depth, in particular near the continental borders of France, solutions made from the regional seismic networks are taken as preferential solutions in the SI-Hex catalogue. In addition to some solutions coming from a study devoted mainly to the west of France and referred to as LDG [Nicolas *et al*., 1990], three zones of preferred solutions are defined in the 2014 version of the catalogue: 1) the French Alps; 2) the southernmost Alps and Mediterranean domain, including Corsica; and 3) the Pyrenees. An additional fourth zone is added by taking the hypocentre locations calculated by Arroucau [2006] in the Armorican massif for the period 1980-2004 (see fig. 3a). When an event is not present in one of the regional catalogues, the solution of the national backbone catalogue is kept (SI-Hex solutions). A fifth zone, northeastern France, is scheduled for a future issue of the SI-Hex catalogue. The processing techniques used by the laboratories in charge of the regional catalogues all differ but they share the same 1D Hypoinverse-type iterative least square inversion scheme.

French Alps (Sismalp)

The regional study by Thouvenot *et al*. [2013] supplements and updates an earlier one presented by Thouvenot and Fréchet [2006]. It covers the period 1989-2009 and the geographical frame shown in figure 3a. It is directly linked to the Sismalp network operated by OSUG in Grenoble [Thouvenot *et al*., 1990]. The original arrival times from the Sismalp network are completed by the bulletin data from LDG and RéNaSS in France, and Genoa in Italy. The area where the highest hypocentres location accuracy is expected is shown in figure 3b.

Hypocentre locations are performed with the Hypref code, an algorithm modified from Hypo71 [Lee and Lahr, 1975] for the Alpine seismicity [Fréchet, 2005]. This code is designed for millisecond processing of arrival times and it takes into account secondary arrivals and the station elevations for the ray computation. The 1D regional model with a Vp/Vs ratio of 1.7 is given in table II. Weights are applied to the stations in order to favour stations close to the epicentre. They vary linearly from 4 at 0 km to 1 at 50 km and are linearly dying to 0 between 50 and 500 km.

Sismalp selection criteria are azimuthal gap smaller than 180°, number of seismic phases larger than 5, nearest

TABLE I. – Seismic velocity model used in the hypocentre localization procedure for the backbone catalogue (adapted from Rothé and Peterschmitt [1950]).

Layer	Depth, km	P velocity, km/s	S velocity, km/s
Upper crust	0-20	5.9	3.4
Lower crust	20-30	6.5	3.7
Upper mantle	>30	8.2	4.4

TABLE II. – Seismic velocity model used for the Sismalp region. No sedimentary layer is present in this model.

Layer	Depth, km	P velocity, km/s	S velocity, km/s
Uppermost crust	0-3	5.30	3.12
Upper crust	3-27	5.92	3.48
Lower crust	27-35	6.60	3.88
Upper mantle	>35	8.00	4.71

station at less than 30 km, and arrival-time residuals smaller than 1.5 s, RMS.

Applying these criteria reduces the number of events from 22,120 to 11,197 in the Sismalp geographic zone. However, about 67% of the discarded events proved to be poorly located quarry blasts, which are of no interest for the purpose of the SI-Hex project.

The southern Alps and the Mediterranean zone (Geoazur)

The regional study by Béthoux [2013] covers the period 2001-2009 and the geographical frame [6°E-9°E, 42°N-44.2°N] (see fig. 3c). This study is referred to as the Geoazur study. As the northern part of this zone overlaps the Sismalp zone, the Geoazur solution is preferred when available, if not, the Sismalp location is kept. The data set is made of various sources. Arrival times from Sismalp, LDG, RéNaSS and Genoa are completed by new arrival time picks from the French strong motion network (RAP) and some broadband stations (TGRS-RLBP from CNRS/Nice University).

Hypocentre locations are performed with the 1D Hypocenter code of Lienert *et al.* [1986]. The 1D P-velocity model given in table III is determined from the regional stations following the method of Kissling [1988]. S-velocities

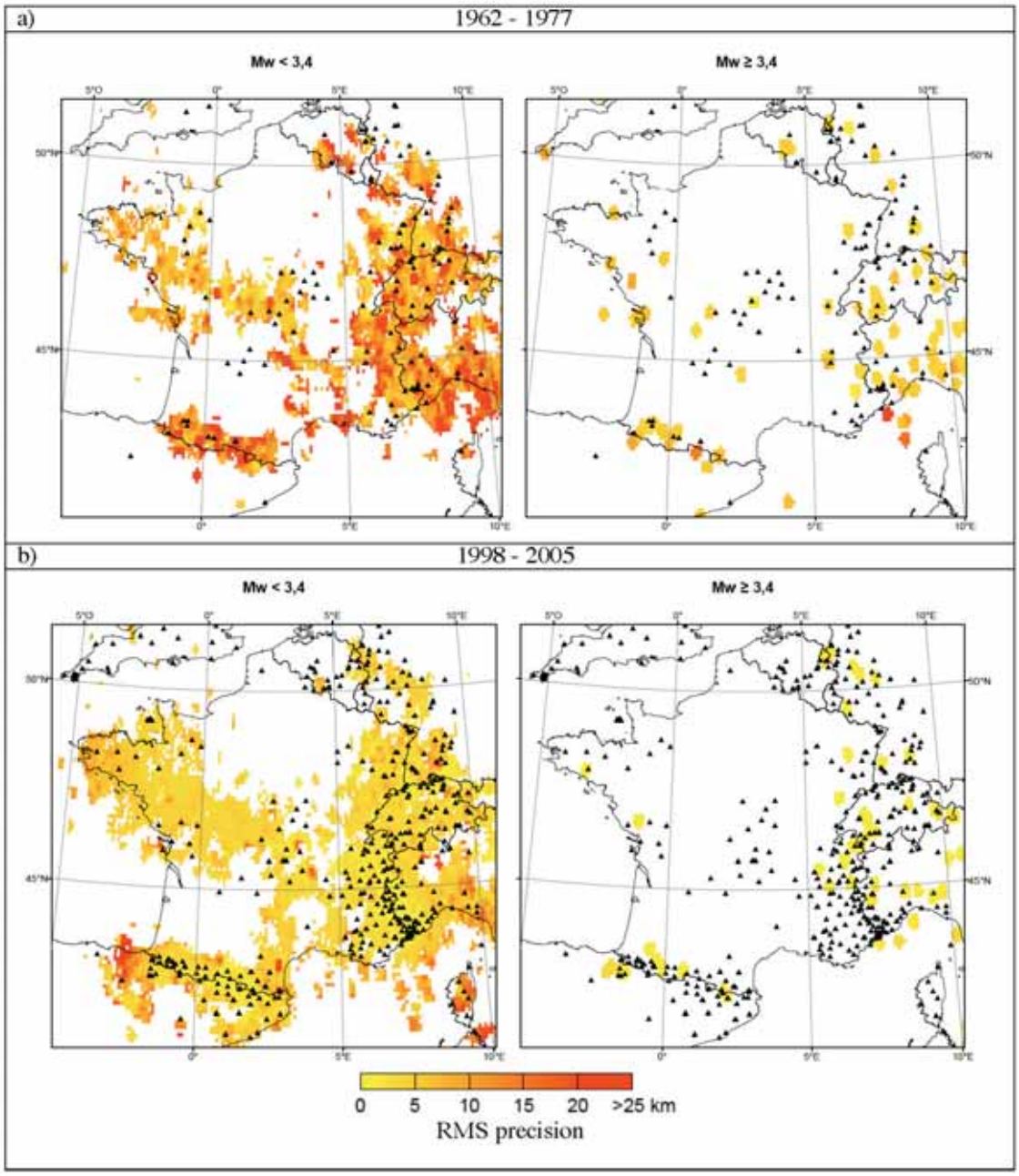

FIG. 2. – Example of RMS precision of the computed epicentre location in the SI-Hex backbone catalogue. For each event, the radius of the circle with an area equal to the standard deviation ellipse is calculated. Precisions shown here correspond, for each 0.1°x 0.1° pixel, to the averaged circle radius of the events located within a distance of 0.2° from the centre of the pixel. Precision varies with time according to the evolution of the network. Figures 2-a and 2-b correspond to the time periods of figure 1. Precision also varies with the magnitude-dependent number of stations used for each location (left $M_w < 3.4$, right $M_w \geq 3.4$).

are computed with a Vp/Vs ratio of 1.74. No weights are applied to the stations but only the local stations are used.

Strong lateral heterogeneities of the crustal structure occur within the southern Alps and the transition from continental to oceanic crust at the Ligurian sea margin. This makes the 1D seismic velocity model a poor representation of the 3D structure. In the framework of the SI-Hex project a 3D velocity structure modelling combined with hypocentre location is developed in order to improve the accuracy of epicentre and depth parameters but in the present 2014 issue of the catalogue, only locations based on the 1D regional velocity model (table III) are reported as preferential solutions.

TABLE III. – Seismic velocity model used for the southern Alps and the Mediterranean zone. No sedimentary layer is present in this model.

Layer	Depth, km	P velocity, km/s	S velocity, km/s
Uppermost crust	0 - 1	4.99	2.87
Upper crust	1-3	5.71	3.28
Upper crust	3-5	5.77	3.32
Middle crust	5-10	6.04	3.47
Lower crust	10-25	6.10	3.51
Upper mantle	25-32	7.50	4.31
Upper mantle	32-40	7.79	4.48
Upper mantle	>40	8.11	4.66

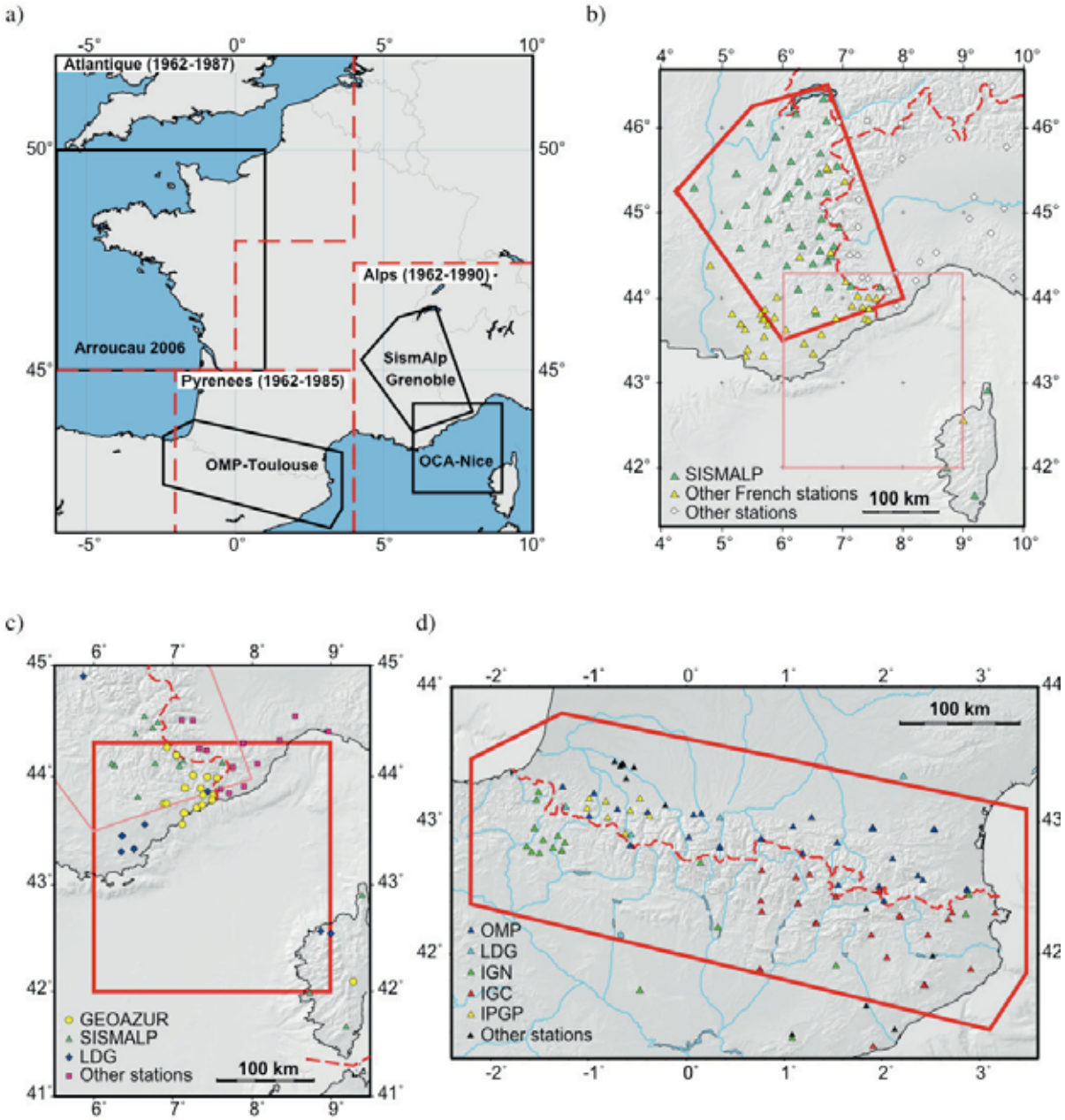

FIG. 3. – Four zones of preferential location solutions of the 2014 version of the SI-Hex catalogue (inset 3a); 3b: Alpine zone (Sismalp, Grenoble); 3c: Mediterranean zone (Geoazur, Nice); 3d: Pyrenees zone (OMP, Toulouse). Geoazur solution is preferred in the overlapping area between zones b) and c). Symbols represents the stations used to compute the preferential location whether they are inside or outside the outlined zones (red polygones).

The Pyrenees

The regional study by Sylvander [2013] covers the period 1997-2009 and the area south of the line running from [2.4°W-43.8°N] to [3.6°E-43.0°N] (see fig. 3d). Over the 1996-2000 period, the OMP network was equipped with homogeneous instrumentation including 3 components 1 Hz velocimetric sensors. Around 70 stations from the OMP, the Spanish IGN, and the Catalonian IGC networks are used for arrival-time phase picking.

Hypocentre locations are performed with Hypo71 [Lee and Lahr, 1975] and the 1D regional P-velocity model given in table IV. This model validated for the whole Pyrenean range is determined from seismic profiles [Daignières *et al*., 1981; Njike-Kassala, 1992]. P velocities are converted into S velocities with a Vp/Vs ratio of 1.717. Because the crust strongly thickens from north to south across the North Pyrenean fault, presenting a sharper transition in the western and central part of the range than in its eastern part, use of P_n and S_n phases is tricky near the axial zone. Nevertheless direct P_g and S_g phases are weakly affected by these crustal thickness variations. Therefore the 1D velocity model given in table IV remains valid for computing the direct wave travel times over the whole Pyrenean zone.

In order to favour the local stations in the hypocentre determination, weights are applied to the travel time data. They are set to 1 up to 30 km from the epicentre and decrease linearly from 1 to 0 between 30 and 120 km. Finally, the solution for the location of the hypocentre corresponds to the barycentre of the series of solutions obtained for a set of initial depths selected between 0 and 20 km, i.e. within the seismogenic zone of the crust in the Pyrenees.

At the end of the location process, a quality criterion A to E is attributed to each hypocentral solution, following a procedure adapted from the quality rating implemented in the HYPO71 software [Lee and Lahr, 1975]. This procedure takes into account various indicators of precision, such as the size of the cluster around the barycentre, the number of seismic phases used, the azimuthal gap, the horizontal and vertical errors from the inversion scheme, the hypocentral distance to the source of the nearest station, and the overall rms residual. Local quantitative estimates of the uncertainty of location are available from a comparison with the solution obtained in a 3D-velocity model [Souriau *et al*., 2014]. The results obtained therein show that the average accuracy in earthquake location is about 2-3 km in horizontal and vertical coordinates over the whole range, and even better (< 2 km) in central-western Pyrenees.

MAGNITUDE

One of the main objectives of the SI-Hex project is to build an homogeneous data set in terms of magnitude. To do so, decision was taken to compute the SI-Hex magnitudes from the LDG short-period velocimetric records because LDG has continuously been monitoring seismicity with a standardized network of stations since 1962. A second decision was to move from local magnitude M_L to the seismic moment magnitude M_w as in most of recent seismic-hazard oriented catalogues [e.g. Grünthal and Wahlström, 2012].

Based on these two initial orientations, and because the local magnitudes $M_{L\text{-}LDG}$ present a systematic bias when compared with M_w issued by different laboratories in Europe [Braunmiller *et al*., 2005; Drouet *et al*., 2010; Chevrot *et al*., 2011], it was decided to come back to the original records for all events with $M_{L\text{-}LDG} > 4$. As the geometry of the network has evolved since 1962, only the stations existing since the 1960s are considered for computing the SI-Hex magnitudes (fig. 4). For events with $M_{L\text{-}LDG} \leq 4$, since this procedure could not be applied to the large set of several ten thousands records, conversions from $M_{L\text{-}LDG}$ to M_w are made with another procedure as explained in the following.

TABLE IV. – Seismic velocity model used for the Pyrenean zone.

Layer	Depth, km	P velocity, km/s	S velocity, km/s
Uppermost crust	0 - 1	5.50	3.20
Upper crust	1-4	5.60	3.26
Middle crust	4-11	6.10	3.55
Lower crust	11-34	6.40	3.72
Upper mantle	> 34	8.00	4.65

Large magnitudes: M_w from LDG coda-wave records

As shown by Mayeda *et al.* [1996], use of coda waves seems the most promising approach to determine magnitudes from a sparse network of stations, such as the LDG network in the 1960s (fig. 5). In order to process the coda-wave signals recorded by the 1-Hz LDG velocimetric sensors, we have modelled the attenuation properties of coda-waves for a set of recent events for which M_w is known with good accuracy [Denieul *et al*., 2013]. Once the regional properties of the coda attenuation are known [Denieul *et al*., 2014], coda amplitude can be used to compute M_w after correction for a station factor.

One of the key issues of any coda modelling technique is the choice of the time-window where a good stability of the coda properties is reached. It is easy to limit the duration of the coda according to some acceptable level of noise. A signal-to-noise ratio of 2 is chosen in SI-Hex to limit the coda signal duration. For application to SI-Hex, this confines the coda signal to less than 300 s after the origin time. It is more difficult to fix the beginning of coda waves after the Sg/Lg arrivals. Starting just after the direct Sg/Lg paths, makes the coda window starting before a stable diffusive regime is reached. Conversely, when starting too late, the coda of small earthquakes may remain below the seismic noise level. As a compromise, the beginning of the coda window is fixed at 1.5 times the propagation time of S_MS computed for a crustal thickness of 35 km and an average S-velocity of 3.4 km/s. Doing so, a significant part of the coda records stays above the noise level for most events of $M_{L\text{-}LDG} > 4$.

According to Denieul *et al*. [2014], the envelopes of coda waves recorded by velocimetric 1-Hz sensors *A(t)* can be modelled with a quadratic time-varying exponent term:

$$A(t) = ISG\Omega t^{-\gamma} e^{-\left(\beta_1 - \beta_2 t^2\right)} \quad (1)$$

In this expression, *I* is the instrumental magnification, *S* is a station correction term, *G* is the coda generating term, Ω is the source amplitude, γ is the geometrical spreading factor, while β_1 and β_2 depend on some average coda quality factor within the frequency bandwidth of the instrument. Regional coda-wave properties are analysed by Denieul *et al.* [2014]. A common geometrical spreading factor $\gamma = 0.75$ is

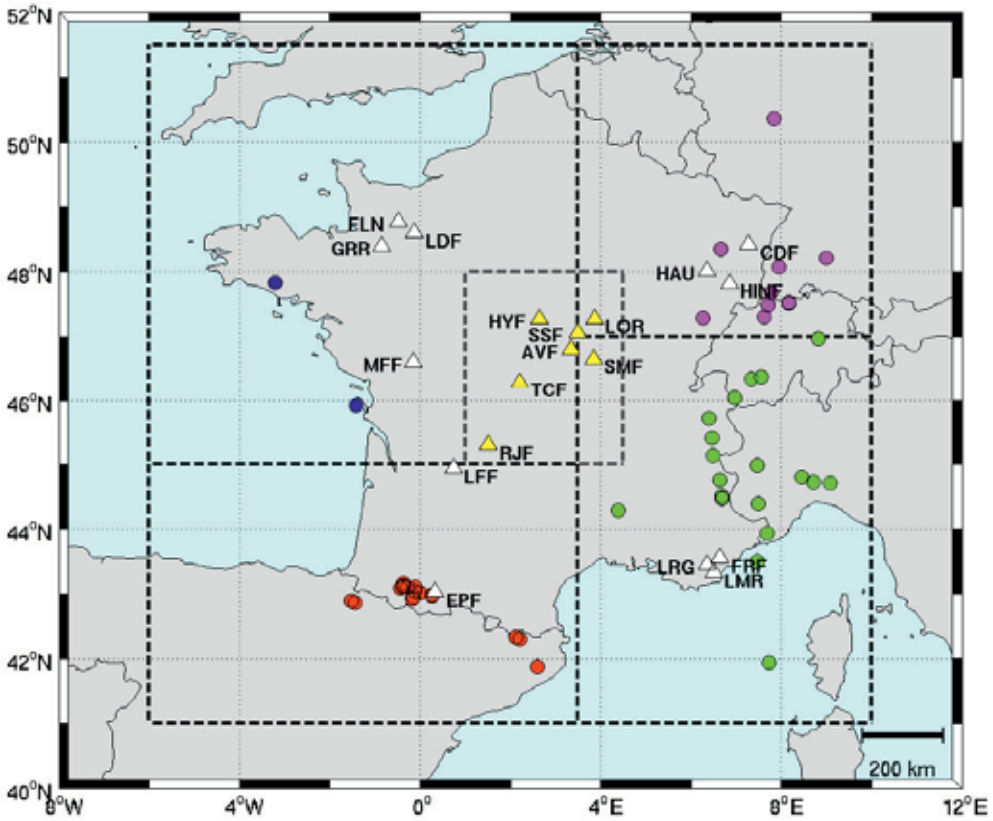

FIG. 4. – Network of LDG stations existing since the 1960s (white and yellow triangles) together with epicentres of the reference events used for M_w magnitude calibration between 1997 and 2013 (circles). Yellow triangles correspond to stations for which a specific modelling of the coda was necessary (see text).

fixed, and the regional attenuation parameters β_1 and β_2 are computed by least-square fitting of the observed coda envelopes. Four regions are considered in metropolitan France according to the broad geological features where both the stations and the events are located (white triangles in figure 4 and table V). The southeastern region includes strong crustal heterogeneities, however, and more refinements would be necessary to better model the coda envelope shape there. In order to limit the heterogeneity of coda properties in this latter region, we have excluded the LDG station located in Corsica for which the coda waves present very different shapes, likely because of the dominant oceanic structure of the crust in the Ligurian sea.

Modelling the coda-waves recorded in the central part of France requires some particular processing (yellow triangles in figure 4). After trying several parameter combinations, we have chosen unique values of β_1 and β_2 whatever the epicentral regions, by adding to the logarithm of the coda amplitude, a correction term C depending on the epicentral region (table V).

Finally, the station correction term S of expression (1) is estimated by averaging the ratio between the coda amplitude at station n and the reference station FLN, as in Campillo *et al.* [1985].

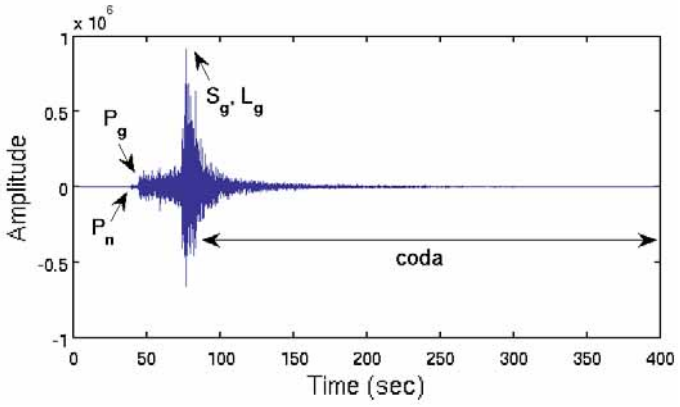

FIG. 5. – Example of regional earthquake coda waves recorded by the LDG 1-Hz vertical velocimetric sensor at station MFF. This $M_{L\text{-}LDG}$ = 5.7 event occurred on September 30, 2002, in the northwestern region near Lorient (M_w = 5.3 according to Perrot *et al.* [2005]; and M_w = 5.2 from the SI-Hex coda method presented here).

TABLE V. – Regional attenuation parameters β_1 and β_2 used to model the coda envelopes when both the stations and the epicentre are located in one of the four SI-Hex regions. For the stations located in the central region (yellow triangle in figure 4), unique values of ß1 and ß2 are used whatever the epicentre location, but a correction term C depending on the source region is added. There is no $M_{L\text{-}LDG}$ > 4 event in the region « Centre ».

Attenuation parameters	North West	North East	South West	South East	Centre
β_1	-13.6 10^{-3}	-18.610^{-3}	-18.9 10^{-3}	-26.2 10^{-3}	-16.3 10^{-3}
β_2	9.4 10^{-6}	16.3 10^{-6}	16.1 10^{-6}	29.7 10^{-6}	12 10^{-6}
C	0.4	0	-0.05	-0.5	-

Once station corrections are made, $IS_{ref}G\ log_{10}(\Omega)$ can be adjusted to M_w by linear regression (fig. 6). For this purpose, we selected a list of reference Mw values for recent events of magnitude ranging between 3 and 5 from Delouis *et al.* [2009], Chevrot *et al.* [2011] and Perrot *et al.* [2005] and different values taken from the website of Geoazur (University of Nice), and SED (ETHZ, Zurich).

The direct conversion of $Log_{10}(\Omega)$ into M_w is applied to all LDG records with local magnitude $M_{L\text{-}LDG} > 4$. Standard deviation of the differences between the predicted and reference M_w is $\sigma = 0.16$. As the records made during the digital period (1997-2009) are processed in such a way that they mimic the analog recording systems based on audio-tape recorders (1977-1996), or the former paper recorders (1960-1976), the same instrumental magnification is used. The same conversion rule thus applies when computing M_w from coda-waves recorded either with the LDG digital recording system or the older analog recorders. The main differences lie in the way the coda amplitude is measured. It is measured directly by least-square fitting of the envelope computed over the full coda-window length during the digital recording period, while prior to 1997, only the high quality parts of the digitized audio-tape records and the measurements made by hand on paper records are used. There is little loss of precision when measuring the envelope amplitude on the digitized audio-tape records, but the measurement errors become larger prior to 1976 during the paper recording period.

Unfortunately, several records of the $M_{L\text{-}LDG} > 4$ events are lost, mainly during the period 1979-1984, or are of too poor quality for applying the coda method in the earliest time. To circumvent the difficulty, a linear regression relationship between the local magnitude $M_{L\text{-}LDG}$ and $M_{w\text{-}coda}$ is established from the 59 reference events that occurred during the digital recording period at LDG (1997-2013). This conversion rule predicts $M_w = 3.4$ for $M_{L\text{-}LDG} = 4.0$, i.e. a magnitude difference of 0.6 identical to that found by Braunmiller *et al.* [2005]. The conversion rule correctly predicts the values of $M_{w\text{-}coda}$ computed from the existing coda records of the period 1979-1984 with no bias and a standard deviation of 0.3 within the SI-Hex zone. When applied to the paper-recording period (1962-1975), this conversion rule based on the recent digital recording period poorly predicts $M_{w\text{-}coda}$. The bias in the prediction reaches half a magnitude unit. For this reason, a different conversion rule based on 49 events for which both $M_{w\text{-}coda}$ and either $M_{L\text{-}LDG}$ or M_{D_LDG} are known is established. This latter conversion rule predicts $M_{w\text{-}coda}$ with no bias but a large standard deviation of 0.4. It is applied to convert M_{LDG} into M_w for a few events, such as the Corrençon/Vercors earthquake of April 25, 1962 in the Alps ($M_{D\_LDG} = 5.3$, $M_w = 5.5$). The only exception to the above rules concerns the large Ligurian offshore earthquake of July 19, 1963, a double event according to Augliera *et al.* [1994]. The conversion rule predicts $M_w = 6.3$ when applied to this $M_{LDG} = 5.9$ earthquake located within the 20 km extension of the SI-Hex zone. Instead of taking this high M_w value in the catalogue we have used the $M_w = 6.0$ determined by Rovida *et al.* [2011] and reproduced by Fracassi *et al.* [2012].

Small magnitudes: M_w converted from $M_{L\text{-}LDG}$

The number of natural events with magnitude $M_w \leq 3.4$ ($M_{L\text{-}LDG} \leq 4$) reaches 37902 within the SI-Hex zone. This number is by far too large for a systematic application of the coda modelling method with visual check of the coda envelopes. Because the source corner frequency of these small events is higher than 3 Hz [Drouet *et al.*, 2010], the

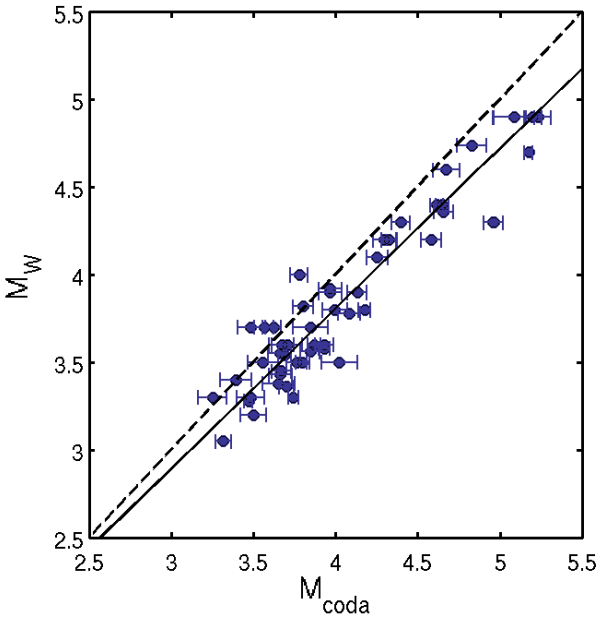

FIG. 6. – Linear orthogonal regression between $M_{coda} = \log_{10}(IS_{ref}G\Omega)$-2 (continuous line) and M_w of reference events which occurred since 1997. The factor 2 is added to roughly correct M_{coda} from the product of the coda generation term G, the reference station site response S_{re} and the instrumental magnification I_0 in order to access the source term Ω. The dotted line would correspond to $M_w = M_{coda}$. Horizontal bars show the standard deviation σ_c of M_{coda} among the different stations. No standard deviation are given for the reference M_w, they are implicitly set equal to σ_c when using orthogonal regression scheme [Castellaro *et al.*, 2006].

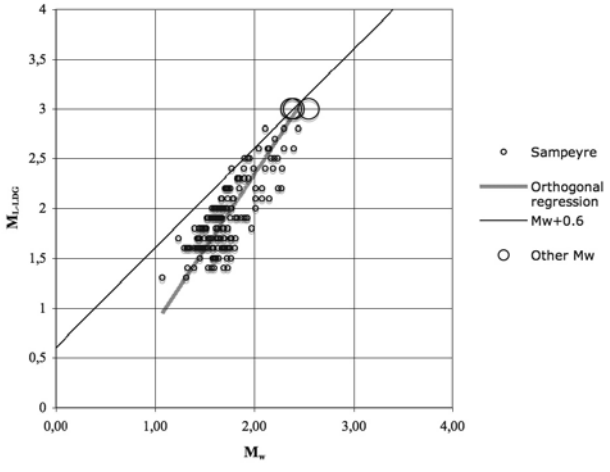

FIG. 7. – Orthogonal linear regression between $M_{L\text{-}LDG}$ and M_w from Godano *et al.* [2013] for the sequence of aftershocks near Sempeyre in the southern Alps, Italy (grey line and small circles). The three large circles correspond to the M_w values predicted for a $M_{L\text{-}LDG} = 3$ earthquake by the relationships of Braunmiller *et al.* [2005], Grünthal [2012], and that of the SED catalogue [Goertz-Allmann *et al.*, 2011] after converting $M_{L\text{-}SED}$ into $M_{L\text{-}LDG}$ from a linear regression based on the Basel geothermal event data. The black line $M_{L\text{-}LDG} = M_w - 0.6$ is the extrapolation of the relationship used in SI-Hex for intermediate magnitudes ($3.117 \leq M_{L\text{-}LDG} \leq 4$).

maximum amplitude of the Sg/Lg phases recorded with the LDG 1-Hz velocity sensors, and thus $M_{L\text{-}LDG}$, can be used safely as a proxy for M_w by applying a linear regression to $M_{L\text{-}LDG}$. As there is no $M_{L\text{-}LDG}$ for some of the events located by the regional networks, additional rules are determined by linear regression in order to convert the values of M_L issued from the different French regional observatories into $M_{L\text{-}LDG}$ [Cara *et al.*, 2013].

From observations and theoretical considerations, the slope of the linear relations between M_L and M_w should be close to unity. However for $M_w < 2$, this rule is no longer valid, due either to attenuation of the impulsive signal generated by the source provoking a reduction of M_L, or to some peculiar physical properties of the source [Deichmann, 2006]. This non-unity slope has been observed several times since the work of [Bakun, 1984]. It was clearly evidenced during the monitoring of the geothermal field sequence of seismic events at 5 km depth in the Basel area [Bethmann *et al.*, 2010] and has been confirmed by several studies, in particular those concerning a similar geothermal field north of Alsace, France [Dorbath *et al.*, 2009] and a large sequence of aftershocks near Sempeyre, Italy, in the southern Alps by [Godano *et al.*, 2013]. In order to convert $M_{L\text{-}LDG}$ into M_w two ranges of magnitude are considered accordingly:

$$M_w = M_{L\text{-}LDG} - 0.6, \quad \text{for } 3.1 \leq M_L \leq 4, \quad (2)$$

$$M_w = 0.664\ M_{L\text{-}LDG} + 0.45, \quad \text{for } M_L < 3.1 \quad (3)$$

The constant of –0.6 we found above at $M_{L\text{-}LDG} = 4$ is identical to the one proposed by [Braunmiller *et al.*, 2005] and the slope of 0.6642 is adjusted to the seismic moment values of the Sampeyre aftershock sequence [Godano *et al.*, 2013] (see fig. 7). The value of 3.117 is chosen in such a way that the rule (3) converting $M_{L\text{-}LDG}$ into M_w is continuous across the $M_{L\text{-}LDG} = 3.117$ boundary.

DISCRIMINATION

The initial choice of the SI-Hex project to collect a set of data as exhaustive as possible led to include in the database events identified by numerous monitoring centres in which the discrimination procedures are strikingly different. This heterogeneity in discrimination procedures is highlighted in table VI, which shows the number of events supplied by four seismic centres for three types of events. Although the series of reported events are different, the ratios between the different types obviously show that the labels "*ke*" (*known earthquake)*, "*uk*" (*unknown earthquake),* and "*km*" (*known mine)* are differently interpreted by these centres. Consequently it is clear that the different centres have not the same policy for characterizing an event as artificial or not.

Among the different artificial seismic events that we had to identify, most of them are quarry blasts. Although a

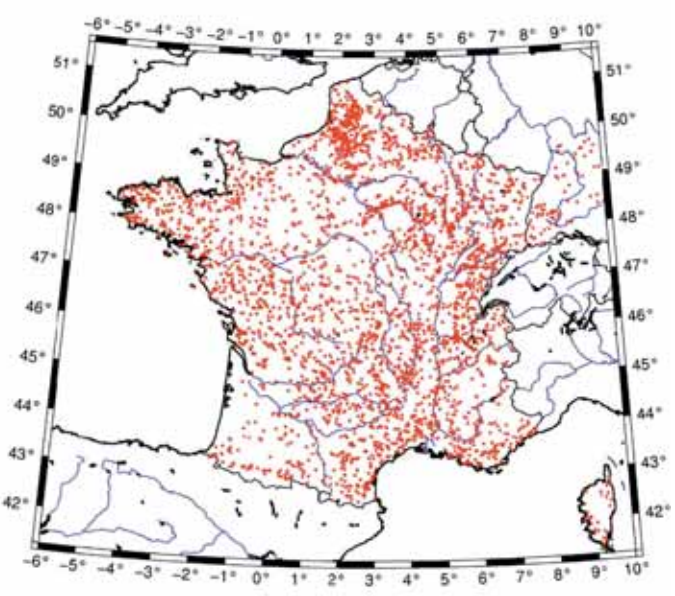

FIG. 8. – Map of identified quarries of hard rocks merged from informations of "Bureau de Recherches Géologiques et Minières" and the "Ministère de l'environnement et du dévelopement durable". Those quarries are potentially seismogenic but not all of them produced seismic events.

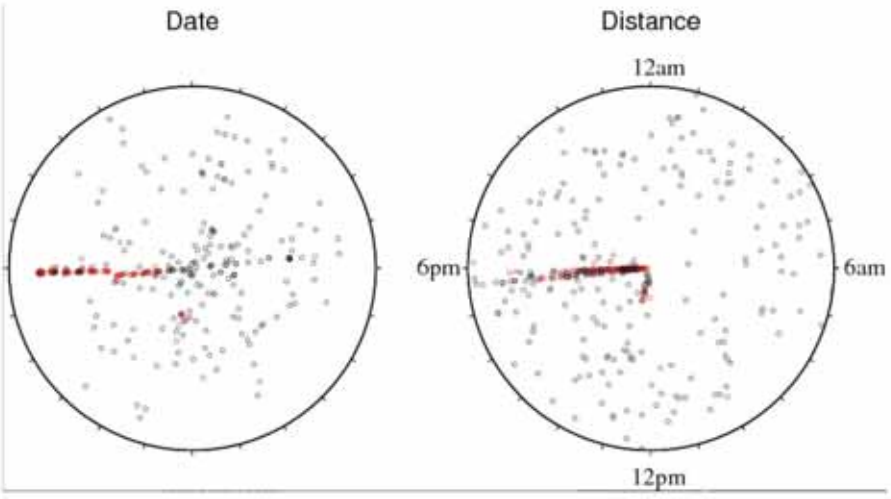

FIG. 9. – Polar representation of events located around the Luzenac (Pyrenees) mine, the polar angle showing the local time of the events. Red dots are identified as "km" and black dots as "ke" in the original database [Godey *et al.*, 2013]. Left: radius proportional to the date of the events since 1967 with clustering during summer. Right: radius proportional to the distance from the center of the mine, (42.806 N; 1.802E) from 0 to 20 km. Note that the quarry blasts occurr mainly shortly before 6 pm and a secondary cluster after 12 pm.

TABLE VI. – Number of events identified as known earthquake ("ke"), unknown ("uk") and known mine ("km") by four major contributors to the original SI-Hex database and related percentage.

Laboratory	ke	uk	km	Number of reported events
LDG - Arpajon, FR	42 544 82%	2 633 5%	6 730 13%	51 907 100%
MDD - Madrid, E	11 160 43%	1 417 5%	13 650 52%	26 227 100%
RéNaSS - Strasbourg, FR	20 166 96%	745 4%	11 0%	20 922 100%
SED-Zurich, CH	410 6%	6 337 94%	8 0%	6 755 100%

good knowledge of the active quarries that could generate seismic signals has been acquired during the SI-Hex project as shown by the map of figure 8, their number (more than 4,400) is too large to allow a direct association of seismic events and quarries by using location information only.

In a more general approach, merging discrimination information associated with arrival-time analyses coming from several monitoring centres leads us to merge events declared as different types by the different centres. For these reasons, we cannot rely on the declared types only and we searched a more elaborate discrimination scheme for application to the SI-Hex project. Two main areas of research are explored:

– a statistical study of the spatiotemporal distribution of the events, the objective being to highlight regions where an important number of events takes place at nearly the same time along the year;

– a study of digital recordings, in order to define criteria allowing us to check the choices made by the analysts of the monitoring centres.

Statistical analysis

An example of spatiotemporal distribution of events is shown in figure 9 where a set of events is located at distances less than 20 km from the Luzenac open-air quarry (Pyrenees). Each event is represented by its rank in the database (radius) and its daily origin time (polar angle). Red dots are "*km*" events and black dots are "*ke*" as labelled in the original bulletin. All the "*km*" events exhibit the same origin-time, but an important number of "*ke*" events also occur at the same time, strongly suggesting that these

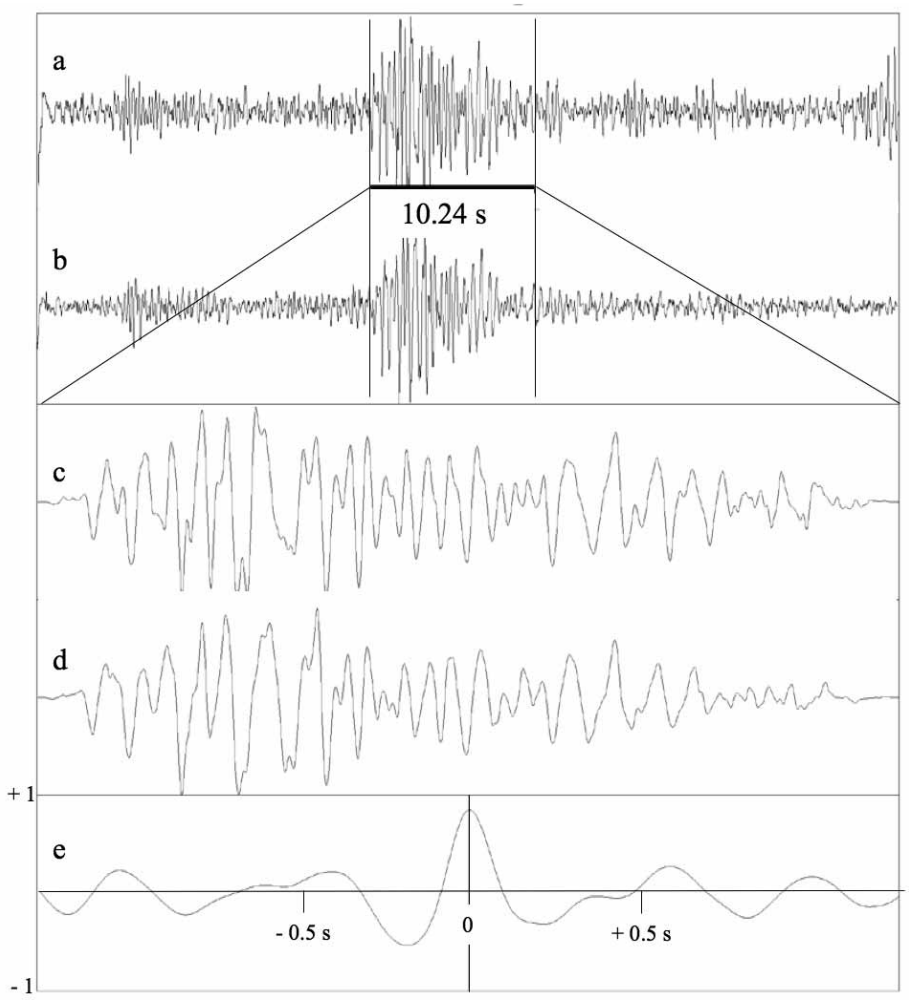

FIG. 10. – Example of very similar events, which are labelled as different types in the original database but are likely to share the same origin: waveforms of October 24th 2005 (a) and December 13th 2002 (b) events recorded at OG14 Sismalp station; c) and d), zoom of the S-wave signal over which the cross-correlation is computed; e) cross-correlation function between c) and d).

events are also man-made events. Such an analysis performed at the level of regional observatories allows the analyst to identify quarry blasts among the series of seismic events. However, such a statistical approach cannot provide a perfect discrimination procedure as some of the quarry blasts may occur at different times.

Signal processing techniques

In order to make a more reliable discrimination between events, correlation techniques are applied when possible. Figure 10 shows the signals of two events, which were assigned a different types in the original database (two upper traces), and their correlation (bottom trace). The similarity of the two signals highlighted by their high correlation level clearly indicates that they are likely to have been generated by the same type of event.

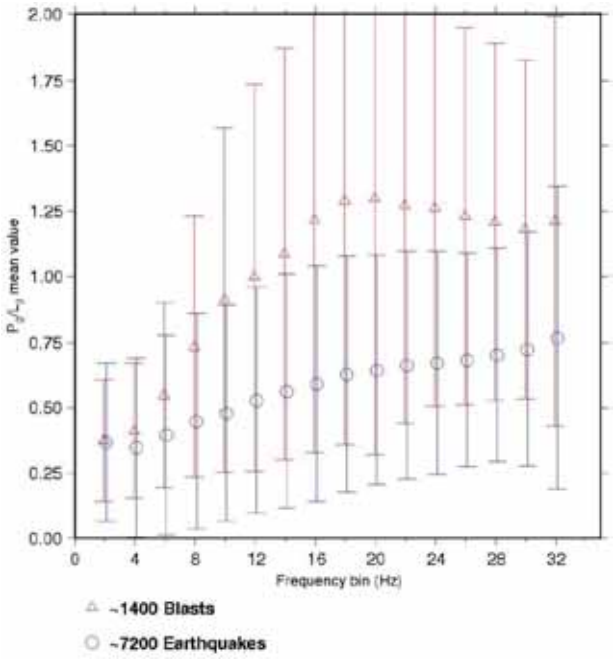

FIG. 11. – Example of numeric criterion which helps for discrimination: the ratio of Pg/Lg amplitude as a function of frequency is discriminating for frequencies greater than 10 Hz at short distances (OMP application to events in the Pyrenees).

Among the numerous criteria, which have been tested by different observatories, the ratio of energy between P-type and S-type waves is certainly one of the most efficient. However, applying this method needs a tuning of different parameters, such as the frequency bands of analysis for example, at the regional scale. Two techniques are investigated:

– use of the spectral ratio of Lg vs Pg waves which is discriminating for frequencies larger than 10 Hz. Combining this information with the origin-times then leads to an automatic discrimination criterion with less than 10% of misclassification. This technique is applied to the database of OMP (Toulouse), which spans the period 1997 to 2009 (fig. 11);

– fitting the spectral ratio of Lg vs Pg waves by a regression line for each event. Its slope and the value of the spectral ratio at a reference frequency determine another discrimination criterion. Figure 12 shows the application of this criterion to the LDG database for central France. It results again in an efficiency of about 90%.

A rather independent problem is the identification of marine explosions. It led us to develop specific signal

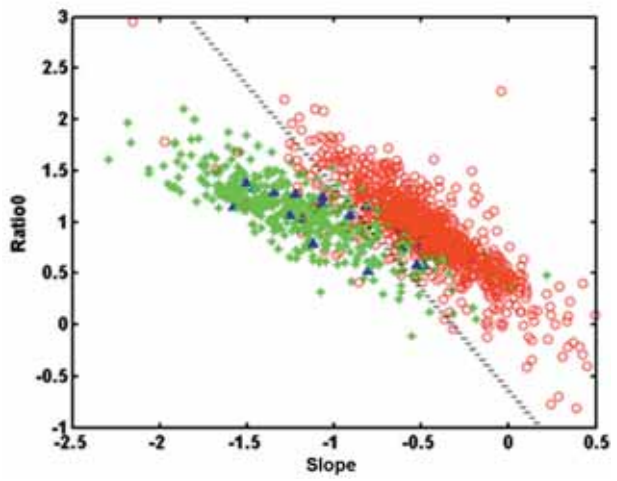

FIG. 12. – Example of numerical criterion which helps for discrimination: for each event, the Lg/Pg spectral ratios are fitted by a line represented by its slope. The amplitude of the spectral ratio at a reference frequency is plotted versus the slope. Green symbols: "km", red symbols: "ke"; blue symbols: "uk" in the original database. The dotted line is the discrimination line (LDG application to events in central France).

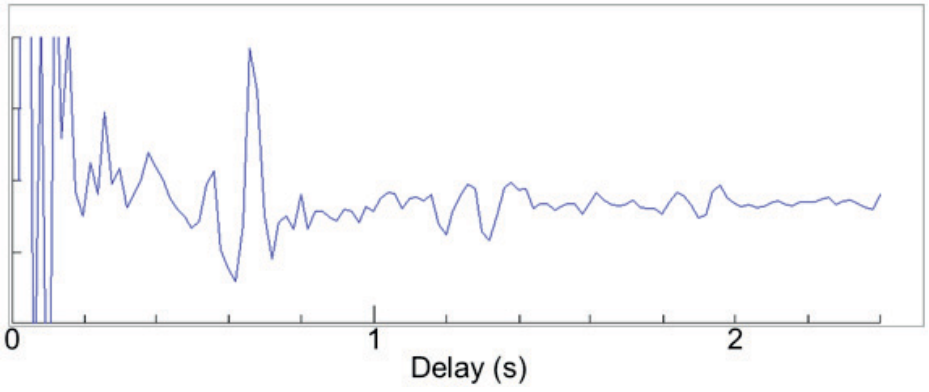

FIG. 13. – Example of cepstrum analysis on a record for a marine explosion showing the echo (delay = 0.63 s) associated to the bubble pulse.

processing techniques which are relevant for item 1) in the SI-Hex strategy described below. Even though most of the events in the SI-Hex database are located inland, the choice made at the beginning of the project to extend the area of interest to 20 km off the marine zone encompassing the whole French exclusive economic area (the "SI-Hex zone") implies the incorporation of a large number of explosive events detonated under sea-level on the continental platform. As for quarry shots, official information about these events are difficult to obtain, leading to studies dedicated to the identification of physical effects on seismic records. The main idea is that underwater explosions result in a pulsatile source due to the expansion/compression of the gas bubble. This well-known effect generates interferences, which can be detected on the records by using signal analysis tools such as cepstrum algorithm. In order to get an automatic tool, we have applied cepstrum analysis combined with the DTW (Dynamic Time Warping) algorithm commonly used in speech analysis. After a learning step based on a selection of events of the two types located close to the shore line, the entire database of events for which waveforms were available at the LDG (since 1996) has been processed, and the results compared to the a priori type chosen by the analysts. Finally, less than 15% of the events are misidentified; all of these are then carefully controlled by a senior analyst who assigns the final type for the SI-Hex database.

Discrimination in the SI-Hex catalogue

Although all these signal processing techniques provide highly valuable information, they cannot be applied to all events of the database because it would necessitate an analysis of small event waveforms not all accessible in the SI-Hex project. Fortunately, because tests run on subsets of events strongly support the validity of the discrimination performed at the regional scale by the different observatories, a pragmatic strategy is applied through the following steps:

1) use signal processing techniques when possible,

2) if not, use the type "*ke*" (known earthquake) or "*se*" (suspected earthquake) provided by the analyst of the regional observatory,

3) events which are not positively selected after step 1) and 2 are eventually considered as artificial.

All the seismic events identified as artificial at the end of the discrimination process are shown in figure 14. After removing these artificial events from a total number of 110,480 seismic events, 50,773 and 38,027 remain in the extended and SI-Hex zones, respectively.

CONCLUSION

The collective work performed within the SI-Hex project by most geophysical institutes dealing with earthquake

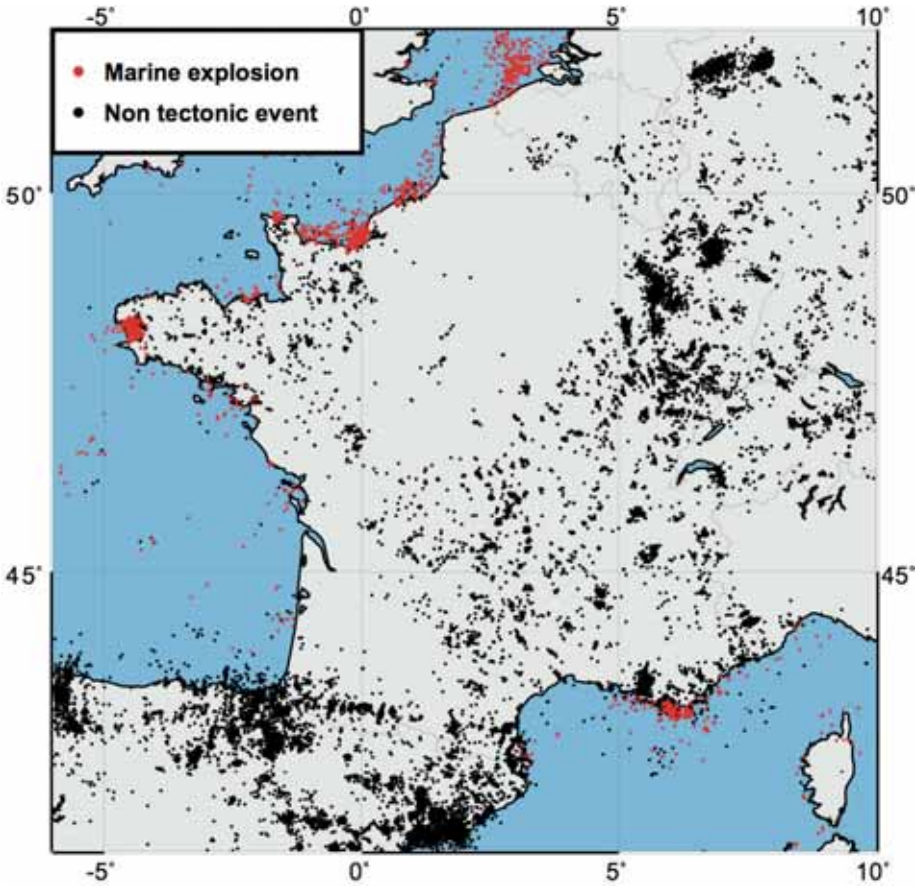

FIG. 14. – Map of identified artificial seismic events in the SI-Hex extended zone.

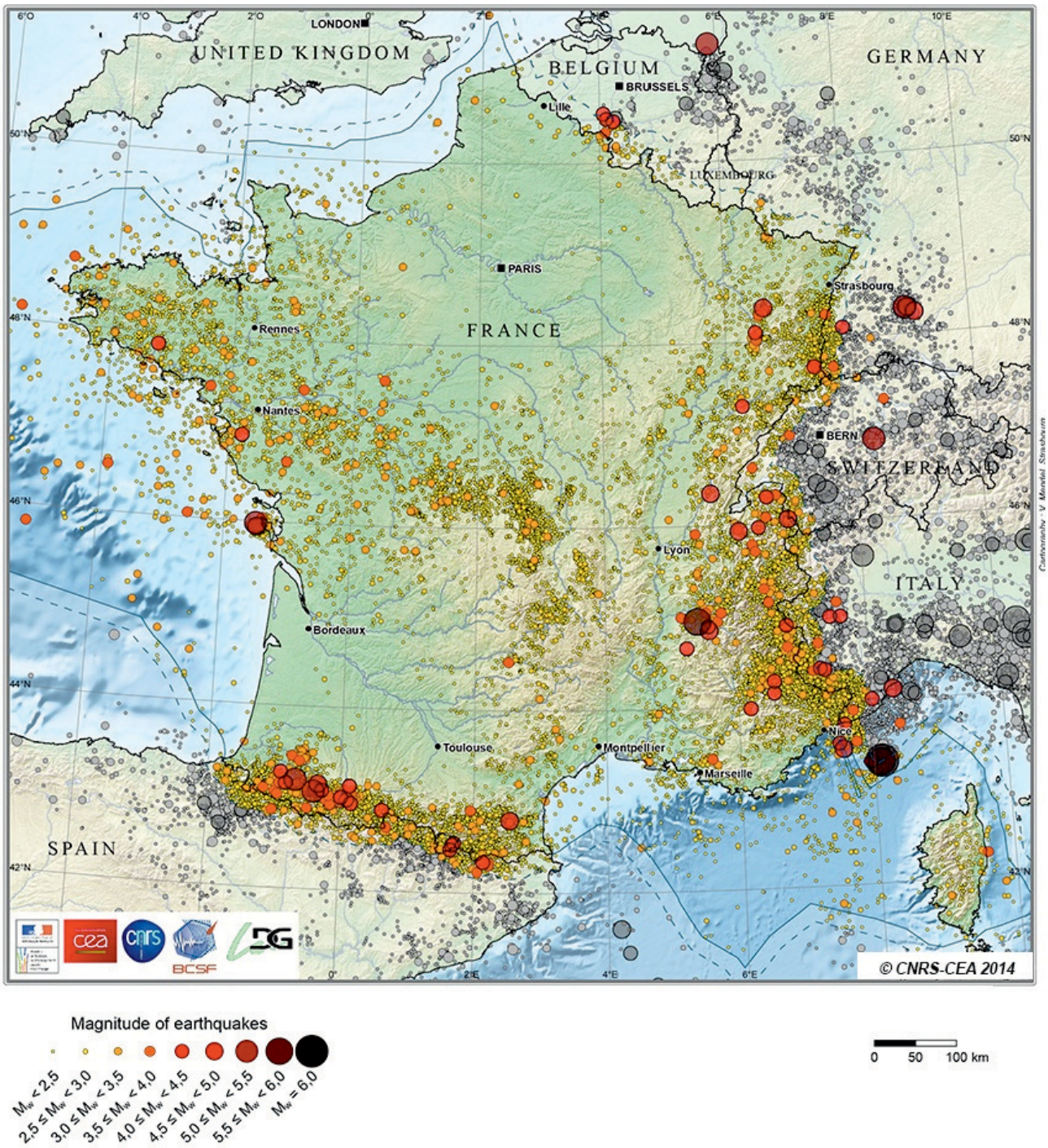

FIG. 15. – Seismicity 1962-2009 of metropolitan France and the surrounding marine exclusive economic zone extended 20 km away to account for maximum location uncertainty (SI-Hex-zone). Coloured symbols show the epicentres located either within the SI-Hex zone, or abroad but felt with EMS-98 intensity I ≥ IV in France (see table VIII). Grey symbols for other events located abroad. Symbol size shown in the inset corresponds to the seismic moment magnitudes M_W within 0.5 intervals. The map illustrates the BCSF-LDG catalogue of seismicity, 2014 version, encompassing 38,027 events remaining after the discrimination step.

monitoring in France significantly improves our knowledge of instrumental seismicity. For the first time all available time-pickings from the different French networks as well as those of the neighbouring countries are used in a unique localization procedure based on an average 1D velocity model to produce a backbone catalogue aimed at identifying all seismic events occurring within metropolitan France and the exclusive marine economic zone between 1962 and 2009. The statistical precision of location evaluated in a unique computational procedure and presented in figure 2 provides a lower bound for location uncertainties of events labelled "SI-Hex" in the database. In addition, better precisions of hypocentre locations are obtained for recent times in four broad areas

TABLE VII. – Number of events per magnitude range and time periods. The M_w magnitude ranges correspond to the main divisions of the procedure used for computing the SI-Hex magnitudes. The time periods correspond to the main steps in the recording procedures (paper, analog magnetic tapes, and digital recording with satellite transmission).

SI-Hex magnitudes	1962-1975	1975-1997	1998-2009	Total
M_w>3.4	34	61	25	120
2.5≤M_w≤3.4	566	1425	480	2471
M_w<2.5	909	13650	20877	35436

TABLE VIII. – SI-Hex magnitudes M_w of earthquakes located outside the Si-Hex zone and felt with EMS-98 macroseismic intensity I ≥ IV.

Year	Month	Day	Country	SI-Hex Mw	Source of information
1995	6	20	Belgium	4.1	coda
2005	5	12	Switzerland	3.3	coda
2005	11	12	Switzerland	3.4	coda
1964	3	14	Switzerland	5.2	coda
1979	7	3	Switzerland	3.9	coda
1984	9	5	Switzerland	3.8	coda
2004	12	5	Germany	4.4	coda
1965	9	19	Germany	3.4	$M_{L\text{-}LDG}$
1969	2	26	Germany	4.7	coda
1970	1	22	Germany	4.8	(*)
1978	9	3	Germany	5.1	coda
2000	4	26	Italy	4.2	$M_{L\text{-}LDG}$
2008	10	24	Italy	4.0	coda
1990	2	11	Italy	4.3	coda
1993	3	15	Italy	3.6	coda
1997	2	24	Italy	3.9	coda
1968	4	18	Italy	4.3	coda
1971	2	1	Italy	4,4	coda
1972	1	18	Italy	4.5	coda
1974	8	5	Italy	3.3	$M_{L\text{-}LDG}$
1980	1	5	Italy	4.4	coda
1981	2	8	Italy	3.7	coda
1992	4	13	Netherlands	5.4	coda

*from EMEC catalogue [Grünthal *et al*., 2012]

where 1D velocity models and data selection criteria are adapted to the regional seismic networks. Combining the backbone catalogue (SI-Hex solutions) and the more precise location provided by the regional institutes allowed us to build the 2014 version of the BCSF-LDG catalogue, giving the best solution of hypocentres available for each earthquake. Obviously, both the number of events and the accuracy of location improved with time as more stations became available (see table VII).

Another main result of the SI-Hex project is to compute M_w for all events of the catalogue. The source of data used for computing M_w are mostly LDG waveforms for $M_L > 4$ events (coda method) and conversion from M_L into M_w for smaller magnitude events, whether M_L are issued by LDG or other French observatories. A homogeneous procedure is applied to the whole catalogue, solving the problem of discrepancies in magnitude evaluations among the different sources.

Finally, an important effort is made for the discrimination between natural and artificial events. Even when the identification of non-anthropogenic events is not exhaustive and homogeneous over the whole 1962-2009 period, this 2014 version of the BCSF-LDG catalogue greatly improves our knowledge of natural seismicity in metropolitan France. The epicentres and magnitudes of these events are shown on the map displayed in figure 15 accessible from the BCSF web site *www.franceseisme.fr.*

The new BCSF-LDG catalogue represents an efficient tool for future seismic hazard analysis and seismotectonic studies in metropolitan France. Its homogeneous magnitude distribution should, for example, greatly help assessing statistical inferences on earthquake occurrence. Concerning seismotectonic studies, it is important to recall that focal mechanism determination for small crustal events strongly depends on the accuracy of hypocentre locations. More accurate determination of depth and magnitude, as available in the SI-Hex catalogue also will make easier waveform inversions, as carried out in several studies [Perrot *et al*., 2005; Delouis *et al*., 2009 and Chevrot *et al*., 2011].

Several studies presently in progress will allow us to further improve the accuracy of hypocentre locations in two regions where strong lateral heterogeneities of the crustal structure occur, the Alpine-Mediterranean area and the Pyrenees, where 3D localizations are currently being tested. These 3D techniques should in particular allow us to reduce the uncertainty in hypocentral depths. Another improvement, both in location precision and identification of natural events, is expected in the northeastern region between France and Germany, thanks to a regional study performed by Fréchet [2013]. Most of these improvements will be available with the 2015 version of the BCSF-LDG catalogue. Independently, in order to allow the end users to study into more details the seismicity of metropolitan France, the various locations and magnitudes issued by the different observatories will be available on-line through an open multi-origin database, after a complete check of the database is completed. In the forthcoming years the catalogue should be regularly updated by including the ongoing seismicity, thanks to a joint effort of the academic institutions under the BCSF umbrella and CEA/LDG.

Acknowledgments. – The seismicity catalogue issued from the SI-Hex project was made possible thanks to the personnels of the observatories and laboratories who operates the seismological networks belonging to CNRS, Universities, and CEA-LDG. We aknowledge all of them for their long-term continuous effort since the early 1960s. The SI-Hex project has been conducted with the contribution of the French Ministry of Ecology, Sustainable Development and Energy, together with CNRS, six Universities, and CEA (conventions n° 0007147 and n° 2100474508). The coda method for magnitude has been developed by Marylin Denieul under a Ph-D grant linked to the SIGMA/EDF research program.
SGF associate editor: Nicolas Bellahsen

Appendix: Institution and seismic network acronyms

BCSF: Bureau Central Sismologique Français/French Central Seismological Bureau

CEA: Commissariat à l'énergie atomique et aux énergies alternatives / French Alternative Energies and Atomic Energy Commission (France)

CNRS: Centre National de la Recherche Scientifique/ National Center for Scientific Research (France)

DAM: Direction des Applications Militaires/ CEA's Military Applications Division

EMSC: Euro-Mediterranean Seismological Center

EOST: Ecole et Observatoire des Sciences de la Terre/geoscience research institute (CNRS/Strasbourg University) (Strasbourg, France)

ETHZ: Eidgenössische Technische Hochschule Zürich/Swiss Federal Institute of Technology in Zurich

Geoazur: Geoscience research institute (CNRS/Nice University) (Nice, France)

IGC: Institut Geologic de Catalunya/ geoscience research institute (Barcelone, Spain)

IGN: Instituto Geografico Nacional (Madrid, Spain)

INSU-CNRS: Institut National des Sciences de l'Univers/ Geoscience institute of CNRS (France)

IPGP: Institut de Physique du Globe de Paris/ geoscience research institute (Paris, France)

IPGS: Institut de Physique du Globe de Strasbourg/ geoscience research institute (CNRS/Strasbourg University) (Strasbourg, France)

ISC: International Seismological Center

LDG or CEA-LDG: Laboratoire de Détection et de Géophysique/ geoscience research institute (CEA) (Bruyères-le-Chatel, France)

MDD: Instituto Geografico y Cadastral (Madrid, Spain)

OMP: Observatoire Midi-Pyrénées, geoscience research institute (CNRS/Paul Sabatier University) (Toulouse, France)

OPGC: Observatoire de Physique du Globe de Clermont-Ferrand/ geoscience research institute (CNRS/ Blaise Pascal University) (Clermont-Ferrand, France)

OSUG: Observatoire des Sciences de l'Univers de Grenoble/ geoscience research institute (CNRS/Grenoble University) (Grenoble, France)

RAP: Réseau Accélérométrique Permanent/ French accelerometric network (Grenoble, France)

RéNaSS: Réseau National de Surveillance Sismique/French National Seismic Survey (Strasbourg, France)

RESIF: Réseau Sismologique Français/French Seismological Network (Grenoble, France)

RLBP: Réseau Large-Bande Permanent/ Permanent broad-band network (RESIF component, Strasbourg & Nice, France)

SED: Schweitzer Erdbeben Dienst/Swiss Seismic Survey (Zurich, Switzerland)

SI-Hex: Sismicité Instrumentale de l'Hexagone/Instrumental Seismicty for metropolitan France.

Sismalp: Réseau sismologique des Alpes / Seismic Survey of the Alps (Grenoble, France)

TGRS: Très Grande Résolution Sismique / Very High Seismic Resolution (Nice, France).

References

Arroucau P. (2006). – Sismicité du Massif armoricain: relocalisation et interprétation tectonique. – Thèse Sci., Nantes, 194 p.

Aubert G., Bordet C., Massinon B. & Schlich R. (1982). – Surveillance de la sismicité actuelle – réseau français d'observation. La définition et la prise en compte des risques sismiques. *In*: Rap. Groupe CODER, 34-45, Acad Sci., Gauthier-Villars.

Augliera P., Béthoux N., Deverchère J. & Eva C. (1994). – The Ligurian sea: new tectonic evidence. – *Boll. Geofis. Teorica ed Appl.,* **36**, 141-144.

Bakun W. (1984). – Seismic moments, local magnitudes, and coda-duration magnitudes for earthquakes in central California. – *Bull. Seismol. Soc. Am.*, **74**, 439-458.

Béthoux N. (2013). – Région PACA: contribution OCA, Nice. *In*: Rapport final SI-Hex, Annexe A-V, 124-143. – Document en dépôt à la bibliothèque de l'EOST.

Bethmann F., Deichmann N. & Mai P. (2010). – Scaling relations of local magnitude versus moment magnitude for sequences of similar earthquakes in Switzerland. – *Bull. Seismol. Soc. Am.,* **101**, 515-534, doi 10.1785/0120100179.

Braunmiller J., Deichmann N., Giardini D., Wiemer S. & SED Magnitude Working Group (2005). – Homogeneous moment-magnitude calibration in Switzerland. – *Bull. Seism. Soc. Am.,* **95**, 58-74.

Campillo M., Plantet J.-L. & Bouchon M. (1985). – Frequency dependent attenuation in the crust beneath central France from Lg waves: data analysis and numerical modelling. – *Bull. Seism. Soc. Am.,* **75**, 1395-1411.

Cara M., Cote A., Durand J., Granet M., Hoang Trong P. & Holl J.M. (1986). – Le réseau national de surveillance sismique (RéNaSS). – *Bull. Liais. Lab. P. et Ch.*, **143**, 30-39.

Cara M., Denieul M., Sèbe O., Cansi Y. & Delouis B. (2013). – Catalogue principal, magnitudes de moment. *In*: Rapport final SI-Hex, Annexe A-IV, 42-73. – Document en dépôt à la bibliothèque de l'EOST.

Castellaro S., Mulargia F. & Kagan Y.Y. (2006). – Regression problems for magnitudes. – *Geophys. J. Int.*, **165**, 913-930.

Chevrot S., Sylvander M. & Delouis B. (2011). – A preliminary catalog of moment tensors for the Pyrenees. – *Tectonophysics,* **510**, 239-251.

Daignières M., Gallart J. & Banda E. (1981). – Lateral variation of the crust in the north Pyrenean zone. – *Ann. Géophys.*, **37**, 435-456.

Deichmann N. (2006). – Local magnitude, a moment revisited. – *Bull. Seismol. Soc. Am.*, **96**, 1267-1277.

Delouis B., Charlety J. & Vallée M. (2009). – A method for rapid determination of moment magnitude M_W for moderate to large earthquakes from the near-field spectra of strong-motion records (MWSYNTH). – *Bull. Seismol. Soc. Am.*, **99**, 1827-1840.

Denieul M., Sèbe O. & Cara M. (2013). – Crustal coda wave properties in France and magnitude calibration. – IASPEI meeting, Götheborg, July 22-26, 2013 (abstract).

Denieul M., Sèbe O., Cara M. & Cansi Y. (2014). – M_W from crustal coda waves recorded on analog seismograms. – *Bull. Seismol. Soc. Am.* (submitted).

DORBATH L., CUENOT N., GENTER A. & FROGNEUX M. (2009). – Seismic response of the fractured and faulted granite of Soultz-sous-Forêt (France) to 5 km deep massive water injections. – *Geophys. J. Int.*, **177**, 653-675, doi: 10.1111/j.1365-246X.2009.04030.x

DROUET S., COTTON F. & GUEGUEN PH. (2010). – Vs30, κ, regional attenuation and M_W from accelerograms: application to magnitude 3-5 French earthquakes. – *Geophys. J. Int.*, **182**, 880-898.

FRACASSI U., DI BUCCI D., RIDENTE D., TRINCARDI F. & VALENSISE G. (2012). – Recasting historical eartquakes in coastal areas (Gargano promontory, Italy): insights from marine paleoseismology. – *Bull. Seismol. Soc. Am.,* **102**, 1-17.

FRÉCHET J. (2005). – Hypref. – http://sismalp.obs.ujf-grenoble.fr/ftp-sismalp/unix.

FRÉCHET J. (2013). – Région grand Est. *In*: Rapport final SI-Hex, Annexe A-V, 76-89. – Document en dépôt à la bibliothèque de l'EOST.

GODANO M., LARROQUE C, BERTRAND E., COURBOULEX F., DESCHAMPS A., SALICHON J., BLAUD-GUERRY C., FOURTEAU L., CHARLÉTY J. & DESHAYES P. (2013). – The October-November 2010 earthquake swarm near Sampeyre (Piedmont region, Italy): a complex multicluster sequence. – *Tectonophysics*, **608**, 97-111.

GODEY S., BOSSU R. & GUILBERT J. (2013). – Improving the Mediterranean seismicity picture thanks to international collaborations. – *Phys. Chem. Earth*, **63**, 3-11.

GOERTZ-ALLMANN B.P., EDWARDS B., BETHMANN F., DEICHMANN N., CLINTON J., FÄH D. & GIARDINI D. (2011). – A new empirical magnitude scaling relation for Switzerland. – *Bull. Seismol. Soc. Am.*, **101**, 3088-3095.

GRÜNTHAL G. & WAHLSTRÖM R. (2012). – The European-Mediterranean Earthquake Catalogue (EMEC) for the last millennium. – *J. Seismol.*, **16**, 535–570. doi: 10.1007/s10950-012-9302-y.

KISSLING E. (1988). – Geotomography with local earthquake data. – *Rev. Geophys.*, **26**, 659-698.

LEE W.H.K. & LAHR J.C. (1975). – HYP071 (Revised): A computer program for determining hypocenter, magnitude, and first motion pattern of local earthquakes. – *U. S. Geol. Surv. Open File Report*, **75**-311.

LIENERT B.R.E., BERG E. & FRAZER L.N. (1986). – Hypocenter: An earthquake location method using centered, scaled, and adaptively least squares. – *Bull. Seismol. Soc. Am.*, **76**, 771-783.

MAYEDA K. & WALTER W.R. (1996). – Moment, energy, stress drop, and source spectra of western U.S. earthquakes. – *J. Geophys. Res.*, **101**, 11,195-11,208, doi: 10.1029/96JB00112.

NICOLAS M., SANTOIRE J.-P. & DELPECH P.Y. (1990). – Intraplate seismicity: new seismotectonic data in western Europe. – *Tectonophysics*, **179**, 27-53.

NJIKE-KASSALA J.D. (1992). – Contribution à l'étude géophysique de la Chaîne pyrénéenne : sismicité et structure lithosphérique. – Thèse Univ. Toulouse, **1982**, 224 p.

PÉQUEGNAT C., GUEGUEN P., HATZFELD D. & LANGLAIS M. (2008). – The French accelerometric network (RAP) and national data centre (RAP-NDC). – *Seismol. Res. Lett.*, **79**, 79-89.

PERROT J., ARROUCAU P., GUILBERT J., DÉVERCHÈRE J., MAZABRAUD Y., ROLET J., MOCQUET A., MOUSSEAU M. & MATIAS L. (2005). – Analysis of the Mw 4.3 Lorient earthquake sequence: a multidisciplinary approach to the geodynamics of the Armorican Massif, westernmost France. – *Geophys. J. Int.*, **162**, 935-950, doi: 10.1111/j.1365-246X.2005.02706.x. – *Corrigendum*, **163**,1136.

ROVIDA A., CAMASSI R., GASPERINI P. & STUCCHI M. (2011). – CPTI11, the 2011 version of the Parametric Catalogue of Italian Earthquakes. – Milano, Bologna, http: //emidius.mi.ingv.it/CPTI.

ROTHÉ J.P. & PETERSCHMITT E. (1950). – Étude séismique des explosions d'Haslach. – *Ann. Inst. Phys. Globe Strasbourg*, **5**, 3e part. Géophysique, 13-28.

SOURIAU A., RIGO A., SYLVANDER M, GRIMAUD F. & BENAHMED S. (2014). – Seismicity in central-western Pyrenees (France): a consequence of the subsidence of dense exhumed bodies. – *Tectonophysics*, http://dx.doi.org/10.1016/j.tecto.2014.02.008.

SYLVANDER M. (2013). – Region Pyrénées: Contribution OMP. *In*: Rapport final SI-Hex, Annexe A-V, 144-155. – Document en dépôt à la bibliothèque de l'EOST.

THOUVENOT F. & FRÉCHET J. (2006). – Seismicity along the northwestern edge of the Adria microplate. *In*: N. PINTER *et al*., Eds, The Adria microplate: GPS geodesy, tectonics and hazards. – Springer, Dordrecht, 335-349.

THOUVENOT F., FRÉCHET J., GUYOTON F., GUIGUET R. & JENATTON L. (1990). – Sismalp: an automatic phone-interrogated seismic network for the western Alps. – *Cahiers du Centre européen de géodynamique et de séismologie*, **1**, 1-10.

THOUVENOT F., JENATTON L., POTIN B. & SANCHEZ O. (2013). – Région Alpes: Contribution OSUG. *In*: Rapport final SI-Hex, Annexe A-V, 94-123. – Document en dépôt à la bibliothèque de l'EOST.